Impacts of global warming of 1.5 ^{0}C, 2.0 ^{0}C and 3.0 ^{0}C on hydrologic regimes in the northeastern U.S.

Ridwan Siddique[1*], Alfonso Mejia[2], Naoki Mizukami[1] and Richard N. Palmer[3]

[1]Research Applications Laboratory, National Center for Atmospheric Research, Boulder, CO, USA.
[2]Department of Civil and Environmental Engineering, Pennsylvania State University, University Park, PA.
[3]Department of Civil and Environmental Engineering, University of Massachusetts Amherst, MA, USA.

[*]Corresponding author: National Center for Atmospheric Research, 3450 Mitchell Lane, FL2, Rm-1015, Boulder, Colorado Phone: +1-817-987-7967
Email: ridwan.siddique@gmail.com

Abstract

Regional climate change impacts show wide range of variations under different levels of global warming. Watersheds in the northeastern region of United States (NEUS) are projected to undergo most severe impacts from climate change in the forms of extreme precipitation events, floods and drought, sea level rise etc. As such, there is high possibility that hydrologic regimes in the NEUS may get altered in the future which can be absolutely devastating for managing water resources and ecological balance across different watersheds. In this study, therefore, we present a comprehensive impact analysis using different hydrologic indicators across selected watersheds in the NEUS under different thresholds of global temperature increases (1.5^0C, 2.0^0C and 3.0^0C). Precipitation and temperature projections from fourteen downscaled GCMs under RCP8.5 greenhouse gas concentration pathway are used as inputs into a distributed hydrological model to obtain future streamflow conditions. Overall, the results indicate that majority of the selected watersheds will enter into a wetter regime particularly during the months of winter while flow conditions during late summer and fall indicate a dry future under all three thresholds of temperature increases. The estimation of time of emergence of new hydrological regimes show large uncertainties under 1.5^0C and 2.0^0C global temperature increases, however, most of the GCM projections show strong consensus that new hydrological regimes may appear in the NEUS watersheds under 3.0^0C temperature increase.

Introduction

Decision making in many areas of water resources are becoming increasingly challenging due to climate change and other anthropogenic activities (Blöschl et al., 2017; Hirabayashi et al., 2013; Milly et al., 2002; Qin et al., 2020). Changing climate and increased warming of the atmosphere are expected to alter the regional hydrological cycle throughout the world, posing many adverse consequences to different sectors of society (e.g. agriculture, ecosystem, hydropower, navigation, water supply) (Van Loon, 2015). The northeastern region of the United States (NEUS) have been projected to be highly vulnerable to climatic changes (Hayhoe et al., 2007; Siddique et al., 2020; Siddique and Palmer, 2020). In particular, water resources and forest ecosystems in the NEUS show close sensitivity to weather and climate dynamics. Warming of the climate and changes in precipitation pattern can threaten the subtle balances between the NEUS' Earth subsystems by changing the characteristics of seasonal streamflow patterns and river ice dynamics, timing of spring runoff, degree of evapotranspiration and snow depth, soil moisture, and climate extremes (i.e. floods and droughts). This means that climate change can adversely impact the hydrological regimes to add more complexity in water management across NEUS (Campbell et al., 2011).

In December 2015, the 21st Annual Conference of Parties (COP21) was held in Paris which is also popularly known as the 2015 Paris Climate Conference. In the conference, the participating nations (more than 180 of them) from all around the world negotiated an agreement on the reduction of climate change impacts calling for necessary actions to limit any future increase in global mean temperature (GMT) to well below 2^0C above pre-industrial levels and to pursue efforts to restrict it to 1.5^0C (UNFCCC, 2015). Such targets for minimizing

global warming were put forward to significantly reduce the risks and impacts of climate change. However, they seem to be overly ambitious at this point of time considering the current policies and future national plans that were submitted by different countries in preparation of the 2015 Paris agreement to reduce greenhouse gas (GHG) emission (Rogelj et al., 2016).

Through Intended Nationally Determined Contributions (INDCs), different countries have spelled out their future targets to restrict GHG emissions, while some countries have also proposed conditional INDCs by mentioning a range of reduction targets. The collective implementation of all INDCs will still lead to a median warming of 2.6-3.1^{0}C by 21st century which is much higher than the targets of 2015 Paris agreement. Due to differences in mitigation strategies and uncertainties regarding future GHG emission policies, it remains unclear whether 1.5^{0}C, 2^{0}C or 3^{0}C of global warming levels can be achieved (Friedlingstein et al., 2014). Therefore, scientists and policy makers in many parts have urged for increased understanding of the possible consequences under different global warming levels (Gosling et al., 2017; Karmalkar and Bradley, 2017a). Additionally, regional warming rates are different than global warming rates which could lead to diverging climate trends at the regional scale. For these reasons, regional climate change impacts to our natural and built environment, and their associated uncertainties, need to be investigated at various levels of global warming. This could provide regional stakeholders with enough quality information to use as guidance for improved policy making and adaptation measures at various stages in the future.

In hydrology, regional climate change studies have thus far been focused on differences between historical and future time periods (Hayhoe et al., 2007). For instance, many of these

studies discuss how climate change impacts (i.e. floods or droughts, precipitation, temperature, runoff, streamflow etc.) will change through a future time period, such as 2071-2100, compared to a base period in the past under different emission scenarios or representative concentration pathways (RCPs). While RCPs are useful to understand risks associated with emission scenarios, they have limitations in determining differences at different warming levels (2^0 C or 3^0 C) (Mitchell et al., 2016). Within the Coupled Model Intercomparison Project (CMIP) experiment, it is sometimes challenging to understand whether anomalies between time periods are due to enhanced global warming or some other driving factor. However, recent studies after the Paris agreement have shifted their focus more towards different warming levels.

Karmalkar and Bradley (2017) have shown that NEUS will be warming at a much faster rate in the 21st century than many other regions in the CONUS. This fast warming trend is likely to impact regional hydrological features, especially in the areas where river runoff are dominated by snow accumulation and melting processes (Barnett et al., 2005). It is possible that due to increased warming, there will be less precipitation in the form of snow, evaporative demand will increase and snow melt will occur earlier than usual. The cumulative effect of all these outcomes in the future can alter the timing of spring runoff and many other seasonal trends.

Hydrological studies that have explicitly utilized Global Circulation Model (GCM) projections to predict future streamflow conditions have already shown increases in seasonal streamflow and winter floods across NEUS (Demaria et al., 2016; Marshall and Randhir, 2008; Siddique et al., 2020). While the outcomes of many of these regional studies are more or less consistent,

there is, however, a lack of consensus among GCM projections regarding possible timelines of these future impacts, or when in the future these changes are likely to take place. More importantly, it needs to be investigated how alterations in regional streamflow conditions and hydrological regimes are associated with different warming levels (Leng et al., 2016; Marx et al., 2018). Such studies are also useful to highlight potential local or regional consequences that can be avoided by limiting global warming by 1.5^0C or 2^0C above pre-industrial levels.

In this study, we provide a comprehensive impact analysis on different hydrological indicators in the NEUS at different global warming level of 1.5^0C, 2^0C and 3^0C. We use downscaled climate projections from 14 GCM to make an ensemble of hydrological simulations from a physically- based distributed hydrological model. Our main goal here is to obtain a robust understanding of the possible regional consequences under different global warming levels. Particularly, we explore whether there are any significant differences in climate change impacts for streamflow conditions across different spatiotemporal scales.

2. Study area

NEUS is one of the more densely populated regions in the United States. As such, the majority of watersheds are under the influence of heavy anthropogenic activities, i.e. water regulations, land use and land cover changes, population growth etc. Climate variabilities in combination with anthropogenic activities may act as a threat to flow regimes in the NEUS watersheds. In this study, we have selected eight different watersheds with different land use and land cover types to investigate future flow regimes. These eight selected watersheds are among the least regulated watersheds of NEUS having basin areas between 12.2~387.16 km^2. We select the

least regulated watersheds in order to facilitate a more accurate calibration of the hydrological models (Figure 1). At regulated sites, flow conditions should be altered where observations merely reflect natural flow conditions. In Table 1, we provide brief descriptions of the watersheds that have been examined in this study.

Table 1. Descriptions of selected watersheds within NEUS.

No.	USGS ID	Location	Area	Lat/lon	Landuse
1	01105600	Old Swamp River 63/1	12.2	42°11’25" 70°56’43	Forest 41% Residential 34%
2	01169000	North River at Shatteckville	230.69	42° 38’18" 72° 43’32"	Forested
3	01162500	Prieastbrook near Winchedon 107/2	49.70	42° 40’57" 72° 06’56"	Mostly forested
4	01176000	Quaboag River near West Brimfield 26/7	387.16	42° 10'56 72° 15'51"	Forested
5	01096000	Squannacook River near West Groton 110/6	173.14	42° 38’03" 71° 39’30"	7.3% imperviousness, 18% permanently protected land area,
6	01095220	Stillwater River near Sterling. 75/3	78.69	42°24'39" 71°47'30"	Mostly undeveloped forest and wetlands
7	01097380	Nasoba Brook near Acton 98/5	33.17	42°30’45" 71°24’17"	25% protected open space, 10% impervious
8	01100600	Shawsheen River near Wilmington 111/4	96.42	42°34’05” 71°12’55”	50% residential, 30% forest

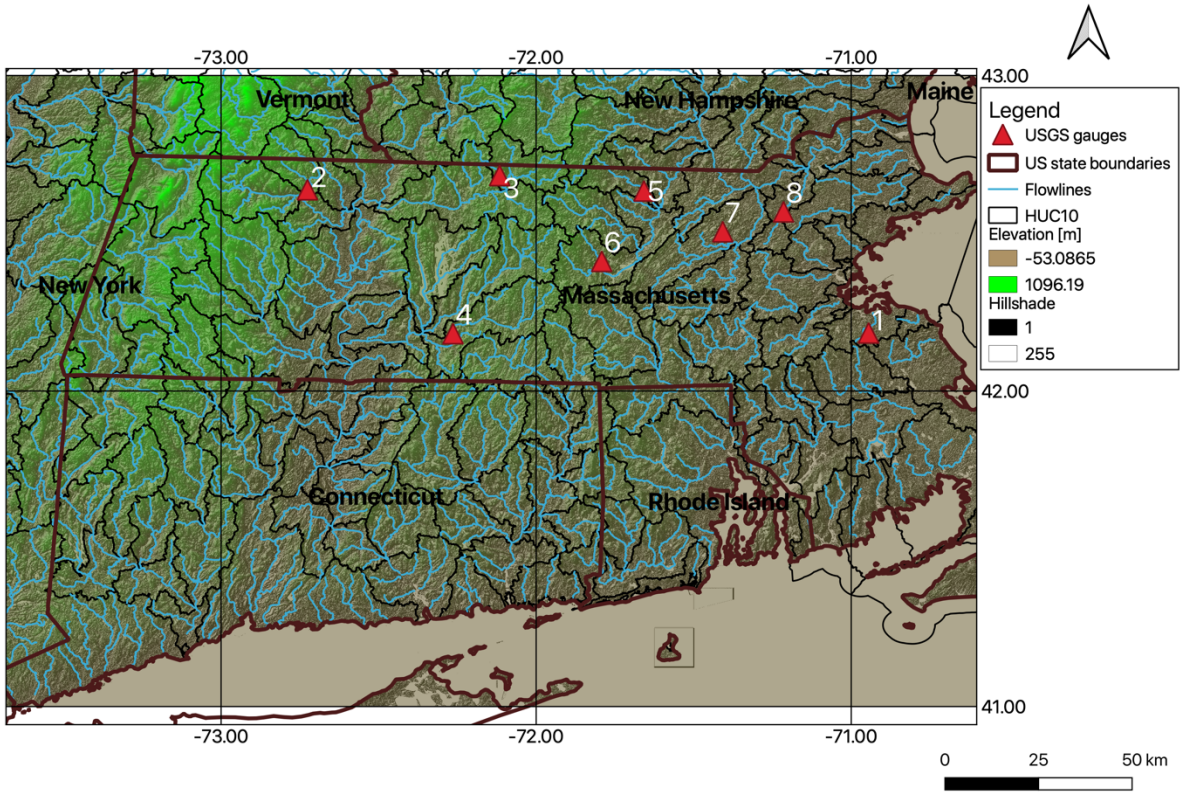

Figure 1. Study watersheds selected in the NEUS.

3. Dataset

3.1 GCM and downscaled output

The set of 14 climate models used in this hydrological modeling effort are selected from the Coupled Model Intercomparison Project Phase 5 (CMIP5; Taylor et al., 2012) ensemble of 36 models under two scenarios: RCP8.5 and RCP4.5 (Meinshausen et al., 2011). The CMIP5 ensemble of 36 climate models (GCMs) and 4 different scenarios captures any of the uncertainties in projections (though the ensemble is not systematically designed for the purpose). While it is ideal to use all available data in production of climate change projections, a careful evaluation of these models is necessary to establish their credibility in providing reliable climate information for the region of interest. The ensemble may also contain redundant information on projections. By combining information on model performance and

similarities in their projections, it is possible to reduce the size of the ensemble without losing critical climate change information.

In this study, we only use a subset of CMIP5 models (14) that were carefully selected for studies of climate impacts in the northeastern U.S. The framework used for their selection is described in detail in Karmalkar et al. (2019) and is based on original coarse resolution GCM data. The model selection involves a thorough assessment of the model performance of 36 CMIP5 models to evaluate their ability to capture key climate features of the northeast U.S. including temperature and precipitation climatology, the annual cycle, variability, and large-scale circulation, facilitating the selection of 10-15 models. The subset of selected models adequately captures the uncertainty in temperature and precipitation projections seen across 36 CMIP5 models, and represent diversity in the spatial patterns of precipitation projections.

Regional projections for the Commonwealth of Massachusetts are produced using the downscaled counterparts of the selected models: the Localized Constructed Analogs (LOCA) downscaled dataset (Pierce et al., 2014). This is a statistical downscaling method (Pierce et al., 2014) that relies on selecting appropriate analog days from observations to downscale coarse-resolution GCM data to finer spatial scales. The LOCA downscaling method has been shown to improve depiction of precipitation extremes over the previous statistical downscaling (e.g., BCSD) methods (Pierce et al., 2014). The LOCA dataset is available at 6-km resolution.

3.2 Observed meteorological and streamflow data

We use multi-sensor precipitation estimates (MPEs) as the observed precipitation data for hydrological model calibration and validation runs. MPEs are produced hourly through the optimal combination of multiple radars and hourly rain gauge data at 4 x 4 km^2 grid resolution

(Zhang et al., 2011). The MPE product used was obtained from the NOAA's Northeast River Forecasting Center (NERFC) and is similar to the NCEP stage IV MPEs (Prat and Nelson, 2015). Gridded MPE products are now widely used in different hydrometeorological applications (Siddique et al., 2015; Yang et al., 2017). Hydrological model used in this study requires gridded temperature observations to obtain monthly potential evaporation and, as input to the SNOW-17 model, to determine snow accumulation and melt. The gridded temperature data were obtained from the NERFC, which generated the data by combining multiple observation networks (METAR, USGS stations, and NWS Cooperative Observer Program). All the gridded data used in this study were resampled using bilinear interpolation onto the regularly spaced grid (4 x 4 km2 cell size) required by HL-RDHM. For the verification of the streamflow simulation and forecasts, daily discharge data from the relevant USGS gauges were used. In total, thirteen years (2004-2016) of streamflow observations were used.

3.3 Determination of 1.5^0C, 2.0^0C and 3.0^0C time periods

We use 14 different GCMs to understand the impact of GCM uncertainties on hydrologic conditions in the NEUS. Different GCMs have different sensitivities to climate forcing and GHG emission scenarios. As such, timelines of mean global temperature increase of 1.5^0C, 2.0^0C and 3.0^0C with respect to pre-industrial conditions will be different among GCMs due to their variations in model initializations, structures and parameterizations. In this study, we have calculated threshold crossing time (TCT) for individual GCMs and a time sampling approach has been implemented (James et al., 2017). This time sampling method has been

241 widely used in other studies as well (Fischer and Knutti, 2015; Marx et al., 2018; Swain and
242 Hayhoe, 2015). A twenty-year running mean global temperature are compared to those of the
243 1981–2000 period in the GCM simulations while 1981-2000 corresponds to 0.9^0C temperature
244 increase with respect to pre-industrial conditions (Karmalkar and Bradley, 2017b). The first
245 20-year period with global warming crossing one of the three warming levels (1.5^0C, 2.0^0C,
246 3.0^0C) is then determined for each of the 14 GCM under RCP8.5 emission scenario. The
247 identified 20-year time period for the corresponding GCM is shown in Table 2.

248 Table 2. Timelines for GCMs to reach different levels of thresholds of temperature increases
249 in the NEUS

Model	1.5^0C	2.0^0C	3.0^0C
MPI-ESM-LR	2012-2031	2030-2049	2058-2077
HadGEM2-ES	2020-2039	2028-2047	2049-2068
CMCC-CMS	2023-2042	2025-2044	2053-2072
MPI-ESM-MR	2015-2034	2023-2042	2053-2072
inmcm4	2038-2057	2050-2069	2078-2097
CanESM2	2009-2028	2022-2041	2043-2062
GFDL-ESM2G	2037-2056	2053-2072	2078-2097
bcc-csm1-1-m	2014-2033	2029-2048	2056-2075
IPSL-CM5A-LR	2009-2028	2023-2042	2043-2062
GISS-E2-R	2027-2046	2047-2066	2080-2099
HadGEM2-CC	2015-2034	2031-2050	2050-2069
CESM1-BGC	2009-2028	2025-2044	2051-2070
bcc-csm1-1	2016-2035	2028-2047	2053-2072
CESM1-CAM5	2022-2041	2034-2053	2049-2068

250
251

252 **4. Methodology**

253 **4.1 Hydrological modeling**

254 The hydrological model selected for this work is NOAA's Hydrology Laboratory-
255 Research Distributed Hydrologic Model (HL-RDHM) (Koren et al., 2004) where the basin is
256 divided into regularly spaced, square grid cells to account for spatial heterogeneity and
257 variability of geophysical conditions. Within HL-RDHM, the heat transfer version of the

Sacramento Soil Moisture Accounting model (SAC-HT) is employed for rainfall-runoff generation, as well as the Snow-17 model to account for snow accumulation and melting. The SAC-HT is a process-based model of the system (conceptual) type which computes freeze-thaw of soil moisture as well as evapotranspiration based on soil temperature (Koren et al., 2014). The SNOW-17 uses near surface temperature to differentiate between snow accumulation or rain at each grid cell and generates snow melt runoff. The runoff generated at each cell is routed through channel and stream networks using hillslope and kinematic wave routing. Overall, a fully distributed HL-RDHM has been implemented at 2x2 km^2 spatial resolution. This particular hydrologic model has been widely applied (Sharma et al., 2018; Siddique and Mejia, 2017; Wood et al., 2016). The model is fully described in (Burnash, 1995).

The hydrological model has been calibrated separately at each of the 8 watersheds. Model calibration in the NEUS watersheds have been a challenge since most of the watersheds in Massachusetts and surrounding states are highly regulated upstream. In total, there are more than 1400 dams in the Commonwealth among which 53 are large and as a consequence, both high and low flows are impacted. Due to such regulations, it was difficult to identify unregulated USGS stream gauge to calibrate the model. For this study, a very careful selection was made to identify eight HUC-8 watersheds that are least regulated based on the existing reports and published documents (Archfield et al., 2009; Armstrong et al., 2008). In this process expert opinion was solicited from USGS. After selecting appropriate sites, the model parameters are calibrated at the selected locations using an automatic calibration technique

called the "Stepwise Line Search" (SLS) over a period of 7 years (2004-2010) after making manual adjustments. Kuzmin et al. (2008) describes the SLS technique in details.

To assess the model performance, we use the following metrics: the correlation coefficient (R), percent bias (PB), and Nash-Sutcliffe efficiency (NSE). Model performance is measured using two different flow conditions: low to moderate flows and high flows. The former represents flows smaller than 25^{th} percentile in the overall flow distribution while the latter represent flows greater than 90^{th} percentile. Through the validation process, it is found that the NSE value for most cases ranges between 0.65~0.85. Besides, PB, for most cases, ranges between 5-10 percent in the sense of absolute value. The range of correlation coefficient varies between 0.75~0.95 which can be considered a high-standard for a physically based hydrological model.

4.2 Hydrologic flow conditions

Anomalies in mean annual flows with respect to long-term mean annual discharge under different thresholds of temperature increases were calculated using the following equation:

$$\text{Anomaly} = (Qi - Qm)/\sigma \qquad (1)$$

where Qi is the annual discharge (mm/WY) in year i; Qm is the long-term mean annual discharge (mm/WY); and σ is the standard deviation (mm/WY). For this study, the three distinct hydrologic flow conditions of dry (anomaly < –0.5), average (–0.5 < anomaly < 0.5), and wet (anomaly > 0.5) years are established based on discharge anomaly.

4.3 Hydrological indicator

As hydrological indicators, we have investigated future changes in magnitude, timing and frequency of mean monthly flow, high and low flows. Mean monthly flows are indicative of available water resources, e.g. for agriculture, water supply, navigation, etc. while high and low flows are indicative of wet and dry conditions.

4.4 Estimation of time of emergence

Climate can change due to both internal and external factors. Internal climate change factors generally include naturally occurring processes like ocean-atmosphere interactions, atmospheric equilibrium and unchanging trends of temperature during pre-industrial time. This type of variations in climate can be termed as Internal climate variations (ICV). On the contrary, external climate change factors include GHG emission, anthropogenic land use and land cover changes etc. which are also known as human induced climate change (HICC) factors. The impacts of ICV on climate change has been widely discussed in recent literature (Deser et al., 2012; Fyfe et al., 2013; Hawkins and Sutton, 2011, 2009) and it has been found ICV will play a significant role in local and regional climate projections especially across near-term (for the years 2010-2060). Many studies have also compared the role of HICC and ICV in future change projections (Giorgi and Bi, 2009; Hawkins and Sutton, 2012; Leng et al., 2016; Zhuan et al., 2018). While investigating relative roles of ICV and HICC on future climate change, Hawkins and Sutton (2012) have identified a process to estimate time when the role of HICC becomes greater than ICV and decided to term it as 'Time of emergence' or ToE. In this study, we have considered ICV as multi decadal variability and estimated ToE over a period of 20 years. Our methodology to estimate ToE is similar to what has been described in Zhuan et al. (2018) except that we have decided to use outputs from one GCM out of fourteen

that gives us the median changes for annual mean streamflow across the years 1980-2099 while Zhuan et al. used ensemble mean of 40 different GCMs to demonstrate ToE. In this study, we have used single GCM (GISS-E2-R) to determine ToE since we wanted to demonstrate the effect of different temperature increases and this can only be done for individual model outputs, not for the mean of a model ensemble. Here, we select GISS-E2-R because it tends to provide the median estimate of future streamflow conditions across selected watersheds. Below we describe step by step procedure to estimate ToE:

1. Using each of the 14-model simulation for the years 1980-2099, we estimate hundred 20-year periods varying by one year, i.e. 1980-1999, 1981-2000, 1982-2001, …., 2080-2099.
2. The 20-year mean value was calculated for each period. A total of 100 mean values were obtained for each climate simulation.
3. The change in streamflow for each of 100 mean values relative to mean value at the reference period (1980–1999) was calculated
4. The median value of these changes which was represented by the model GISS-E2R over 14 simulations was defined as HICC.
5. Using the 14-member ensemble, 100 20-year periods were divided for each ensemble member.
6. The 20-year mean value was calculated for each period and a total of 100 mean values were obtained for each ensemble member
7. The change (relative change for streamflow) in each of the 100 mean values relative to mean value at the reference period (1980–1999) was calculated

8. The standard deviation of these changes over members was calculated for each period and a total of 100 standard deviation values were obtained. ICV was then defined as ±2 or ±1 standard deviations of inter-member differences

With the above steps, 100 HICC values form a curve (GISS-E2-R model) and ICV values form another curve and the intersection of these two curves is defined as the ToE. If an HICC curve intersects an ICV curve of +2 or +1 standard deviations, it implies that there is an increasing climate change trend. If an HICC curve intersects an ICV curve of −2 or -1 standard deviations, then there is a decreasing climate change trend. No intersection implies that HICC does not emerge from ICV or that there is no obvious HICC.

5.0 Results

5.1 Changes in precipitation

Mean areal precipitation in the selected basins of NEUS show significantly different future trends under different threshold of temperature increases. Climate change signal for different seasons are also found to be different. In Figure 2, we show climate change impacts on monthly mean precipitation from fourteen different GCM projections under 1.5^0C, 2.0^0C and 3.0^0C temperature increases where solid lines represent ensemble means of fourteen GCMs and shaded region represent the region of model uncertainty. Future projections in winter months (Dec-Feb) show increases of precipitation under all three thresholds of temperature increases. Largest increases of precipitation during winter are shown under the scenario of 3.0^0C temperature increase which varies between 5~24 percent among different GCMs. Precipitation increases approximately similar for 1.5^0C and 2.0^0C which is around 2~12 percent, although

ensemble mean of fourteen models suggest slightly greater increases for 2.0^0C when compared to increases for 1.5^0C. Increases in precipitation amount during winter may include increases both in liquid rain and snow since GCM projections have shown that number of days above 0^0C will increase in the future across NEUS (Siddique et al., 2020). Thus, different level of temperature increases in combination with increased heavy precipitation events in the future may significantly impact winter peak flows in NEUS watersheds.

During spring months (Mar-May), majority of the GCM projections show increases in precipitation except a few. The range of precipitation increases during spring projected by different GCMs under different warming levels are shown to be approximately similar and ranges between -2~13 percent for different watersheds. Results in Figure 2 also indicates that summer (Jun-Aug) can be the driest season of the year in terms of future decreases in precipitation. Specifically, greatest decreases in precipitation are projected during the months of July and August under 3.0^0C increase in temperature. The ensemble means of GCM projections suggest that decreases are slightly less prominent for 1.5^0C and 2.0^0C although all fourteen GCMs indicate the same climate change signal of decreasing precipitation trends during summer months except June.

Decreases in precipitation are also shown during Fall (Sep-Nov) especially during earlier part of the season. However, model ensemble mean suggests that decreases are slightly smaller compared to summer months and ranges between -2 and -12 percent. Overall, future trends of precipitation under different levels indicate a significant increase in precipitation during winter and spring. Precipitation is projected to decrease across NEUS watersheds during late summer

and earlier months of fall. These change projections in precipitation should have an impact on future flow regimes in the NEUS and adjacent areas.

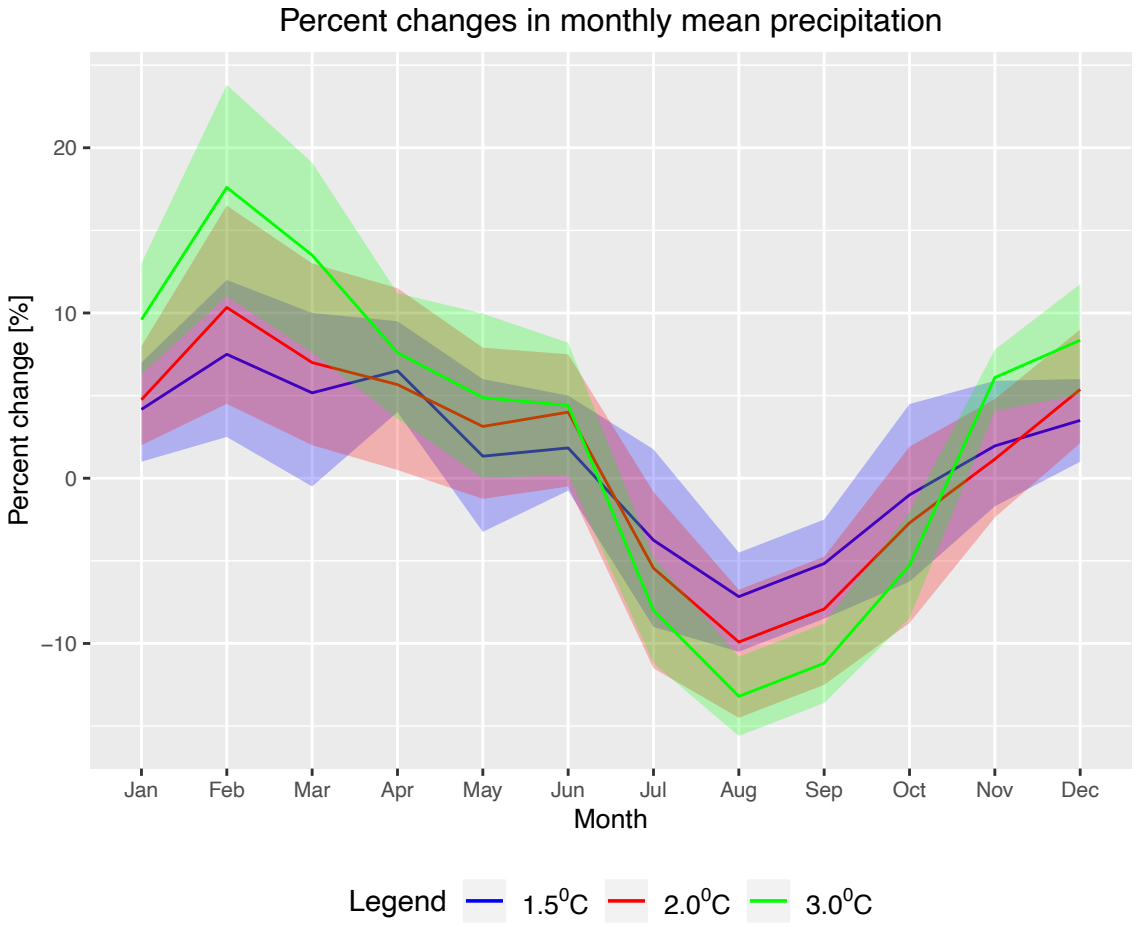

Figure 2. Percent changes in daily mean of monthly precipitation under different levels of temperature increases relative to the base period (1980-1999).

5.2 Changes in streamflow conditions

Magnitude

In this section, we will discuss the impact of climate change on flow regimes in the NEUS which is evaluated for different thresholds of temperature threshold of 1.5, 2 and 3^{0}C. First,

409 mean changes in climatic driving forces are presented to differentiate the causes of change in
410 each of the basin. In Figure 3, we show percent changes in daily mean of monthly flow across
411 all basins for different thresholds of temperature increases. Solid lines represent the mean
412 changes and the shaded regions represent the changes from fourteen GCMs and across all eight
413 basins that has been considered in our study. Apparently, future trends for monthly flows are
414 found to be consistent for different temperature increases. For instance, monthly flow in winter
415 months (December-February) have shown consistent increases for all three thresholds of
416 temperature increases (1.5^0C, 2.0^0C and 3.0^0C). These increases in monthly flows can be the
417 direct influence of potential future increases in winter precipitation. With increased
418 temperature, there will be increased precipitation more in the form of rain than snow. Increased
419 rain events in combination with snowmelt runoff may influence the winter peak flows to rise
420 more in the future compared to the present. Our results in Figure 3 also confirms the same
421 trends where 3.0^0C temperature increase show greater increases in winter flows when
422 compared to 1.5^0C and 2.0^0C temperature threshold. For 3.0^0C temperature threshold,
423 increases in winter flow range between 25~75 percent across all watersheds while 2.0^0C and
424 1.5^0C increases show ranges between 5~30 percent and 0~30 percent, respectively. The
425 greatest increases in winter peak flows are shown during the month of February for all three
426 temperature thresholds.
427
428 In NEUS watersheds, peak flows generally occur during the month of March or April when
429 snowmelt is triggered by increased temperature. In the future, however, spring runoff exhibits
430 a decreasing trend particularly during the month of April. This can be the consequence of
431 earlier snowmelt than normal due to rise in temperature level. More specifically, temperature

increases in the future will cause a shift in the timing of spring runoff which indicates that snowmelt runoff will more likely start around March instead of April and therefore, there will be increases in monthly flows of March, but decreases will occur during April. The magnitudes of changes in April floods are shown to be similar for different thresholds of temperature increases and they range around -5~-15 percent across all basins.

Flows during the summer months have shown mixed results when most of the watersheds across all temperature thresholds have shown small increases in flows particularly for the month of June. However, as time increases in summer, more and more watersheds start to show deceases in flows. The mean changes across all basins show maximum decreases during the month August especially for 1.5^0C and 2.0^0C temperature thresholds. This flow behavior during the months of summer can largely be associated with antecedent soil moisture. Since precipitation is projected to increase during winter and spring, there should be increased amount of soil moisture which may persist through the earlier part of summer helping base flows to exhibit slight increases despite of increasing evaporative demand. As antecedent soil moisture starts to perish due to increased temperature, summer flows starts to show decreases towards the latter half of the season (during the months of July and August).

Maximum decreases of monthly flows are observed during the months of Fall (September-November) when approximately all our study watersheds are found to be getting drier for all three thresholds of temperature increases. These decreases range between 2~-23 percent which shows the effect of lack of precipitation and increases in number of consecutive dry days during spring in the future (Siddique et al., 2020). This also indicates the possibilities of extended

droughts in the northeastern watersheds during late summer and early part of the fall in the future.

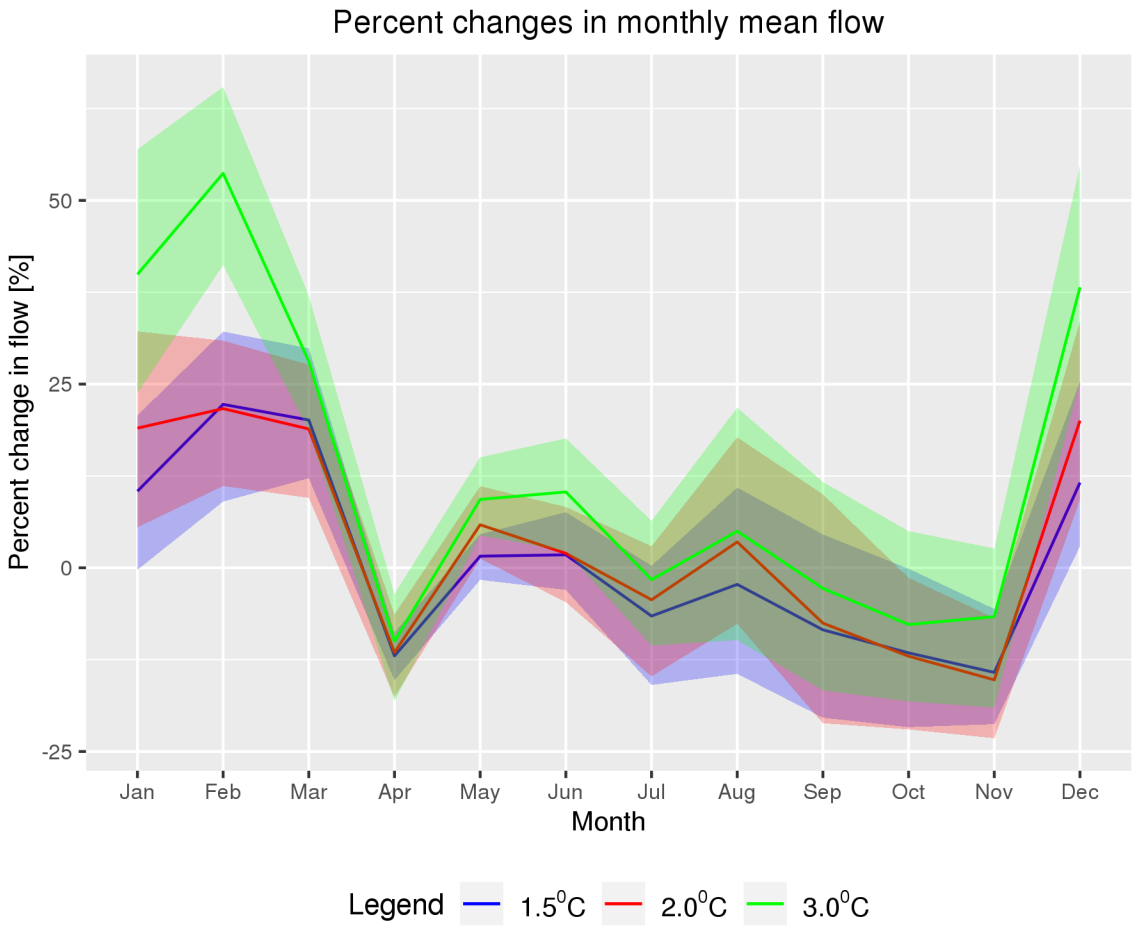

Figure 3. Percent changes in daily mean of monthly streamflow conditions under different levels of temperature increases relative to the base period (1980-1999).

Frequency

In Figure 4, we show timing and frequency of annual peak flows reported by different GCMs under three different thresholds of temperature increases in the future. These outcomes under three thresholds of temperature increases are compared with the outcomes across a base period

466 (for the years 1980-1999). To obtain the results, we have considered all the peak flows greater
467 than 95th percentile in the flow distribution for all fourteen GCMs.
468
469 The results show clear indication of a few possible changes in the frequency and timing of
470 peak flows in the eight different watersheds considered here. First, peak flows during the
471 winter particularly for the month of December and January are shown to be increasing for all
472 three thresholds of temperature increases (1.5^{0}C, 2.0^{0}C and 3.0^{0}C). The maximum increases
473 are shown for 2.0^{0}C increases in the month of January. However, increases are small during
474 the month of February when compared to the base period. The results also show that maximum
475 peak flows generally occur in the month of April during the base period which will see a
476 decrease in the future with increased temperature. On the contrary, the frequency of peak flows
477 is also found to be increasing during the month of March. This is an indication that the
478 frequency of peak flows will increase in the future during the months of winter and early part
479 of spring. With increased temperature there will be increases in extreme precipitation and rain
480 on snow events. Combination of increased rain and snowmelt, thus, may contribute to increases
481 in the magnitude and frequency of runoff and streamflow peaks in the future.

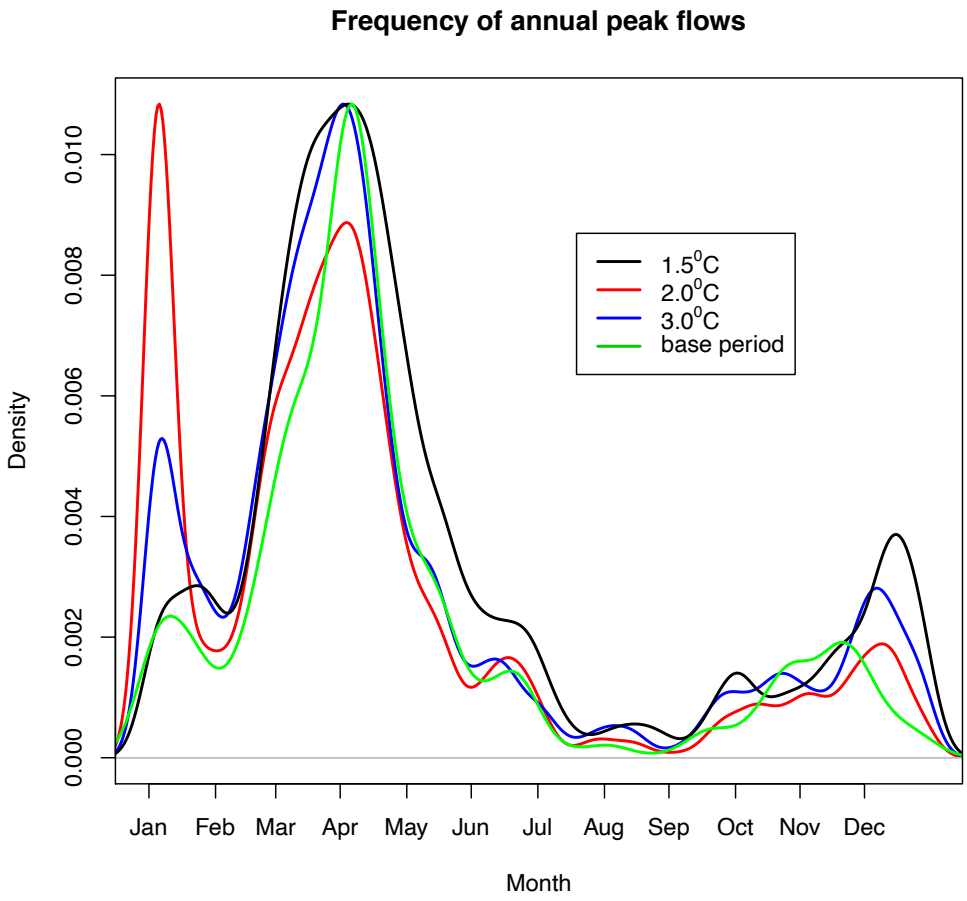

Figure 4. Probability distribution of the timing and frequency of annual peak flow events (above 95 percentiles in the flow distribution) under different levels of temperature increases relative to the base period (1980-1999),

5.3 Anomalies in Hydrological flow conditions

Figure 5 represents average anomalies for different temperature thresholds in the future compared to a base period (1980-1999). Since we have used 14 different GCMs to understand uncertainties, we obtained 14 different realizations of hydrological flow anomalies for each basin. For 1.5^{0}C temperature increase, majority of the GCMs show anomaly values greater

than 0.5 particularly for basins 2-5. An anomaly value over 0.5 means that these basins will enter into a wet regime for mean flow conditions compared to the base period. Two out of eight basins (Basin 1 and 6) show anomaly values around zero for most of the GCMs. This indicates that hydrological flow will remain the same and may not experience any major changes in the future. However, it should be noted that three to four GCMs also report anomaly values less than -0.5 for these two basins which indicates a possible dry flow regime in the future. Since we consider each GCM output an equally likely scenario of the future, we should consider these results carefully as well. For rest of the two basins (Basin 7 and 8), most of the anomaly values range between 0.5 and -0.4 which implies average flow conditions will persist in these two basins. Anomaly results are shown to be almost similar for 2.0^0C temperature increases which also indicate more basins will enter into wet flow regime in the future when compared to the base period. Most extreme cases are found for 3.0^0C temperature increases when six out of eight basins have shown in the future will experience a wetter flow regime. For these six basins, approximately 80 percent of the GCMs report anomaly values greater than 0.5. For rest of the two basins (Basin 1 and 6) show anomaly values between 0.5 and -0.5 indicating average flow conditions (neither extremely dry nor wet) in the future. Overall, our results show that most of the basins in the U.S. northeast may undergo increases in flow conditions due to increased precipitation in this region. However, some GCMs also indicate possible dry future for a few basins especially in the seasons when precipitation is limited.

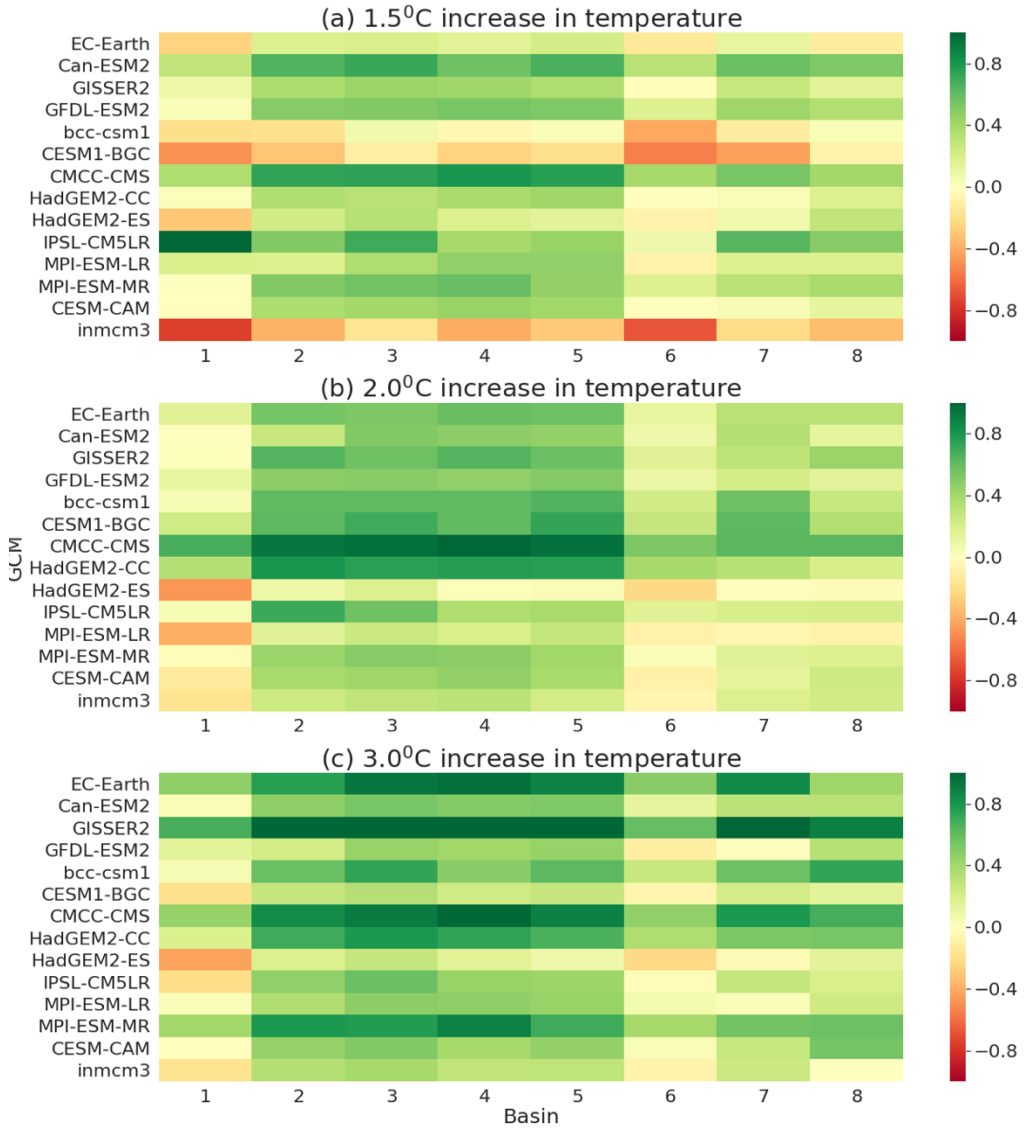

513

514 Figure 5. Average anomalies under different thresholds of temperature increases in the future

515 compared to a base period (1980-1999).

516

517 **5.4 Alteration of hydrologic regimes**

518 In Figure 6 and 7, we have shown time of emergence for annual mean streamflow for basin 1-

519 4 and 5-8, respectively. Here, we have shown results for GISS-E2R model to illustrate regime

520 changes across the years of 2000-2099. GISS-E2R is chosen out of 14 GCMS because it

521 demonstrates median changes for mean annual precipitation across Massachusetts. To produce
522 conservation adaptation strategies, we have used both ± 1 standard deviation and ± 2 standard
523 deviation as ICV. In Figure 6-7, the blue line represents HICC and green and red dashed line
524 represents ICV of ± 1 standard deviation and ± 2 standard deviation, respectively. The
525 intersection of HICC and ICV curve represents the time of emergence of new hydrological
526 regime.
527
528 The results in Figure 6-7 illustrates emergence of new hydrological regimes for both ICV
529 scenarios since HICC curve crosses both ICV curves for 6 out of 8 basins except for basins 1
530 and 6. However, Figure 6-7 cannot provide us with the impacts of different thresholds
531 temperature increases which is the main focus of this study. For this reason, we have
532 summarized results of Figure 6-7 in Table 3 where we have used binary (true/false) variables
533 for basins 1-8 to represent whether new hydrological regimes will occur or not. From the table
534 3, it is evident there are uncertainties regarding ToE for temperature thresholds 1.5^0C and 2.0^0C
535 although we are using a GCM that represent median changes in mean annual streamflow
536 conditions. If we consider a more rigorous ICV of ±2 standard deviation, none of the eight
537 basins report hydrologic regime changes for 1.5^0C and 2.0^0C temperature increases. On the
538 contrary, six out of eight basins (except basin 1 and 6) show regime changes for 3.0^0C
539 temperature increases. For ±1 standard deviation, all eight basins considered here show regime
540 changes for 3.0^0C while six out of eight basins show regime changes for 2.0^0C temperature
541 increase. As ±2 standard deviation is a more robust estimate and there is only 2.3% chance to
542 exceed it, we can say that 3.0^0C temperature increase may have a strong influence behind
543 emergence of a new hydrological regime in the watersheds of northeastern U.S.

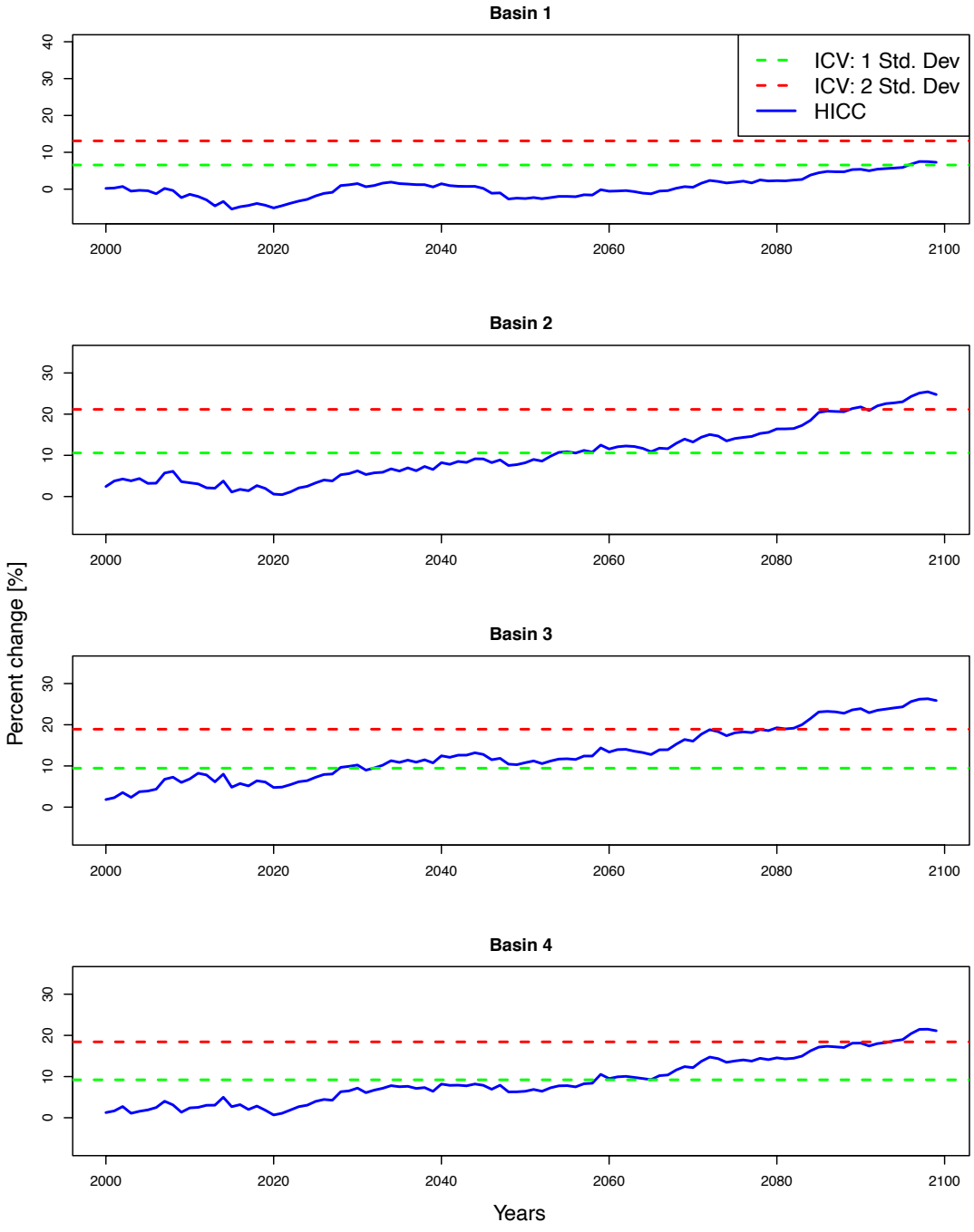

544
545 Figure 6. Time of emergence for mean annual streamflow conditions for watersheds (1-4).

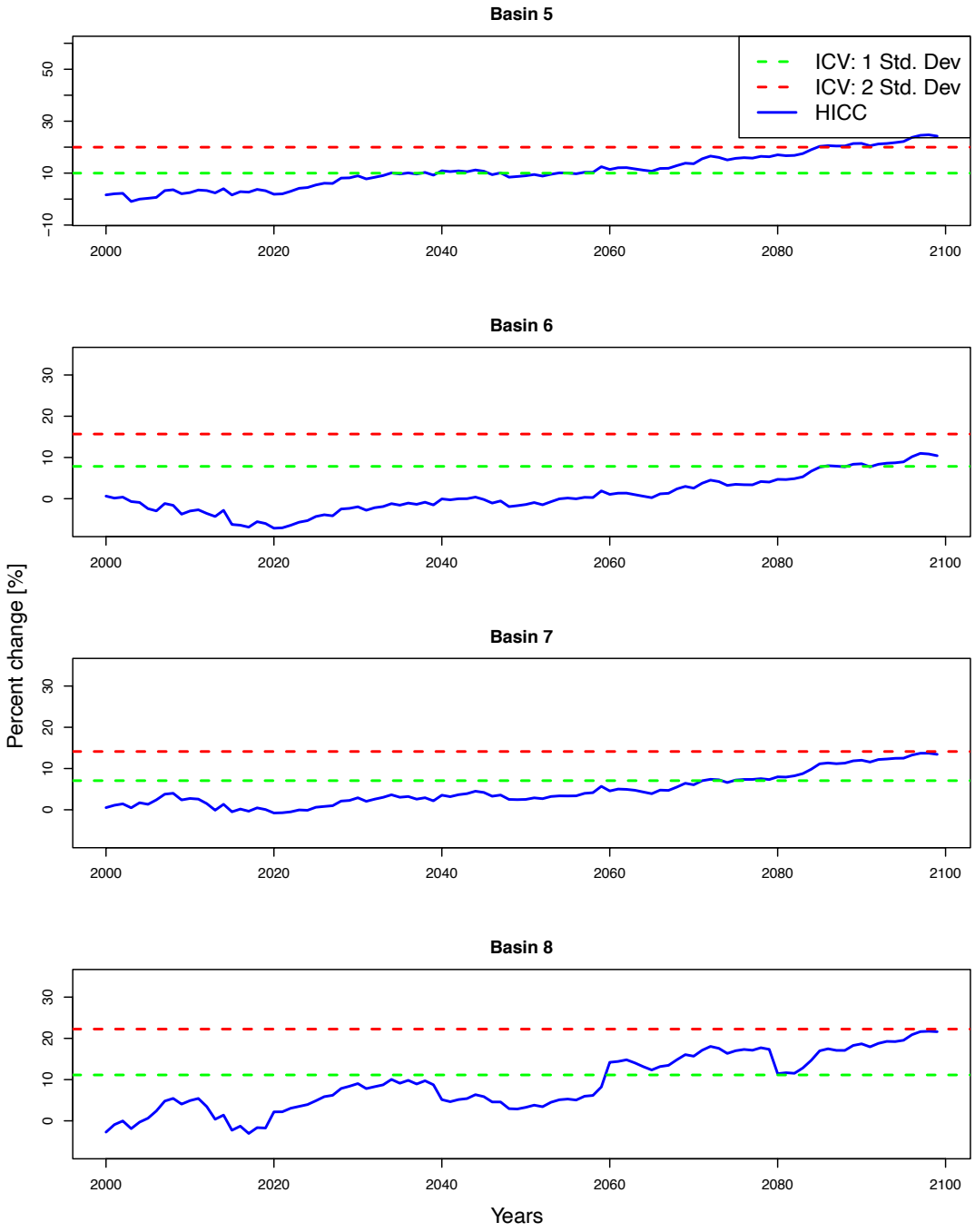

Figure 7. Time of emergence for mean annual streamflow conditions for watersheds (5-8).

Table 3. Summary chart showing whether or not time of emergence will occur under different levels of warming in the NEUS watersheds

	ICV: 1 Std. Dev			ICV: 2 Std. Dev		
	1.5^0C	2.0^0C	3.0^0C	1.5^0C	2.0^0C	3.0^0C
Basin 1	no	no	yes	no	no	no
Basin 2	no	yes	yes	no	no	yes
Basin 3	yes	yes	yes	no	no	Yes
Basin 4	no	yes	yes	no	no	yes
Basin 5	yes	yes	yes	no	no	yes
Basin 6	no	no	yes	no	no	no
Basin 7	no	no	yes	no	no	yes
Basin 8	no	yes	yes	no	no	yes

6.0 Conclusions

For a better understanding of regional climate change impacts and adaptation planning, we need studies targeting local consequences from different levels of global warming. In this study, we used climate projections from 14 carefully selected GCMs to force a physically-based distributed hydrological model to understand future changes in hydrological flow regimes in the watersheds of the northeastern U.S. for different thresholds of global temperature increases (1.5^0C, 2.0^0C and 3.0^0C). Specifically, we have examined eight watersheds in the NEUS with different land use and land cover to explore how anthropogenic activities will have an impact on different quantiles of streamflow conditions (mean, low and peak flow) as well as precipitation in the future under the most extreme GHG emission scenario RCP8.5. The results show large uncertainties regarding hydrologic regime changes under 1.5^0C and 2.0^0C temperature increases. However, it is found that streamflow regimes are likely to change for majority of the watersheds under 3.0^0C temperature increase. The results indicate that most of the watersheds in the future will enter into a wetter regime particularly during the months of winter which will be driven by increased seasonal precipitation. In addition, future

streamflow projections also suggest a drier fall season for most of the basins due to a lack of precipitation and increase of consecutive dry days in the region.

This study utilizes multiple GCM projections to account uncertainties that may arise from meteorological inputs. However, hydrological uncertainties remain unaccounted in this study since we have used the single hydrological model to obtain future streamflow projections. Additionally, uncertainties can also stem from sources like meteorological downscaling, hydrologic model parameters (e.g., land use changes) etc. In future studies, therefore, we recommend to address above mentioned uncertainties to ensure more robust model outcomes. Despite the limitations, this study can provide useful information for local policy makers and stakeholders to setup plans for restricting GHG emission and future climate change adaptations.

Data availability statement: The data that support the findings of this study are available from the corresponding author upon reasonable request.

References

Archfield, S., Vogel, R., Steeves, P., Brandt, S., Weiskel, P., Garabedian, S., 2009. The Massachusetts Sustainable-Yield Estimator: A decision-support tool to assess water availability at ungaged sites in Massachusetts. US Geol. Surv. Sci. Investig. Rep. 5227, 2010.

Armstrong, D.S., Parker, G.W., Richards, T.A., 2008. Characteristics and classification of least altered streamflows in Massachusetts. US Department of the Interior, US Geological Survey.

Barnett, T.P., Adam, J.C., Lettenmaier, D.P., 2005. Potential impacts of a warming climate on water availability in snow-dominated regions. Nature 438, 303.

Blöschl, G., Hall, J., Parajka, J., Perdigão, R.A.P., Merz, B., Arheimer, B., Aronica, G.T., Bilibashi, A., Bonacci, O., Borga, M., Čanjevac, I., Castellarin, A., Chirico, G.B., Claps, P., Fiala, K., Frolova, N., Gorbachova, L., Gül, A., Hannaford, J., Harrigan, S., Kireeva, M., Kiss, A., Kjeldsen, T.R., Kohnová, S., Koskela, J.J., Ledvinka, O., Macdonald, N.,

610 Mavrova-Guirguinova, M., Mediero, L., Merz, R., Molnar, P., Montanari, A., Murphy,
611 C., Osuch, M., Ovcharuk, V., Radevski, I., Rogger, M., Salinas, J.L., Sauquet, E., Šraj,
612 M., Szolgay, J., Viglione, A., Volpi, E., Wilson, D., Zaimi, K., Živković, N., 2017.
613 Changing climate shifts timing of European floods. Science (80-.).
614 https://doi.org/10.1126/science.aan2506
615 Burnash, R.J.C., 1995. The NWS river forecast system-catchment modeling. Comput. Model.
616 watershed Hydrol. 188, 311–366.
617 Campbell, J.L., Driscoll, C.T., Pourmokhtarian, A., Hayhoe, K., 2011. Streamflow responses
618 to past and projected future changes in climate at the Hubbard Brook Experimental
619 Forest, New Hampshire, United States. Water Resour. Res. 47.
620 Demaria, E.M.C., Palmer, R.N., Roundy, J.K., 2016. Regional climate change projections of
621 streamflow characteristics in the Northeast and Midwest U.S. J. Hydrol. Reg. Stud. 5,
622 309–323. https://doi.org/https://doi.org/10.1016/j.ejrh.2015.11.007
623 Deser, C., Knutti, R., Solomon, S., Phillips, A.S., 2012. Communication of the role of natural
624 variability in future North American climate. Nat. Clim. Chang. 2, 775–779.
625 Fischer, E.M., Knutti, R., 2015. Anthropogenic contribution to global occurrence of heavy-
626 precipitation and high-temperature extremes. Nat. Clim. Chang. 5, 560–564.
627 Friedlingstein, P., Andrew, R.M., Rogelj, J., Peters, G.P., Canadell, J.G., Knutti, R., Luderer,
628 G., Raupach, M.R., Schaeffer, M., van Vuuren, D.P., Le Quéré, C., 2014. Persistent
629 growth of CO2 emissions and implications for reaching climate targets. Nat. Geosci. 7,
630 709.
631 Fyfe, J.C., Gillett, N.P., Zwiers, F.W., 2013. Overestimated global warming over the past 20
632 years. Nat. Clim. Chang. 3, 767–769.
633 Giorgi, F., Bi, X., 2009. Time of emergence (TOE) of GHG-forced precipitation change hot-
634 spots. Geophys. Res. Lett. 36.
635 Gosling, S.N., Zaherpour, J., Mount, N.J., Hattermann, F.F., Dankers, R., Arheimer, B.,
636 Breuer, L., Ding, J., Haddeland, I., Kumar, R., 2017. A comparison of changes in river
637 runoff from multiple global and catchment-scale hydrological models under global
638 warming scenarios of 1 C, 2 C and 3 C. Clim. Change 141, 577–595.
639 Hawkins, E., Sutton, R., 2012. Time of emergence of climate signals. Geophys. Res. Lett. 39.
640 Hawkins, E., Sutton, R., 2011. The potential to narrow uncertainty in projections of regional
641 precipitation change. Clim. Dyn. 37, 407–418.
642 Hawkins, E., Sutton, R., 2009. The potential to narrow uncertainty in regional climate
643 predictions. Bull. Am. Meteorol. Soc. 90, 1095–1108.
644 Hayhoe, K., Wake, C.P., Huntington, T.G., Luo, L., Schwartz, M.D., Sheffield, J., Wood, E.,
645 Anderson, B., Bradbury, J., DeGaetano, A., Troy, T.J., Wolfe, D., 2007. Past and future
646 changes in climate and hydrological indicators in the US Northeast. Clim. Dyn. 28,
647 381–407. https://doi.org/10.1007/s00382-006-0187-8
648 Hirabayashi, Y., Mahendran, R., Koirala, S., Konoshima, L., Yamazaki, D., Watanabe, S.,
649 Kim, H., Kanae, S., 2013. Global flood risk under climate change. Nat. Clim. Chang. 3,
650 816–821.
651 James, R., Washington, R., Schleussner, C.-F., Rogelj, J., Conway, D., 2017. Characterizing
652 half-a-degree difference: a review of methods for identifying regional climate responses
653 to global warming targets. WIREs Clim. Chang. 8, e457.
654 https://doi.org/10.1002/wcc.457
655 Karmalkar, A. V, Bradley, R.S., 2017a. Consequences of Global Warming of 1.5 °C and 2

°C for Regional Temperature and Precipitation Changes in the Contiguous United States. PLoS One 12, e0168697.
Karmalkar, A. V, Bradley, R.S., 2017b. Consequences of Global Warming of 1.5 °C and 2 °C for Regional Temperature and Precipitation Changes in the Contiguous United States. PLoS One 12, e0168697.
Karmalkar, A. V, Thibeault, J.M., Bryan, A.M., Seth, A., 2019. Identifying credible and diverse GCMs for regional climate change studies—case study: Northeastern United States. Clim. Change 1–20.
Koren, V., Reed, S., Smith, M., Zhang, Z., Seo, D.-J., 2004. Hydrology laboratory research modeling system (HL-RMS) of the US national weather service. J. Hydrol. 291, 297–318.
Koren, V., Smith, M., Cui, Z., 2014. Physically-based modifications to the Sacramento Soil Moisture Accounting model. Part A: Modeling the effects of frozen ground on the runoff generation process. J. Hydrol. 519, 3475–3491.
Kuzmin, V., Seo, D.-J., Koren, V., 2008. Fast and efficient optimization of hydrologic model parameters using a priori estimates and stepwise line search. J. Hydrol. 353, 109–128.
Leng, G., Huang, M., Voisin, N., Zhang, X., Asrar, G.R., Leung, L.R., 2016. Emergence of new hydrologic regimes of surface water resources in the conterminous United States under future warming. Environ. Res. Lett. 11, 114003. https://doi.org/10.1088/1748-9326/11/11/114003
Marshall, E., Randhir, T., 2008. Effect of climate change on watershed system: a regional analysis. Clim. Change 89, 263–280. https://doi.org/10.1007/s10584-007-9389-2
Marx, A., Kumar, R., Thober, S., Rakovec, O., Wanders, N., Zink, M., Wood, E.F., Pan, M., Sheffield, J., Samaniego, L., 2018. Climate change alters low flows in Europe under global warming of 1.5, 2, and 3° C. Hydrol. Earth Syst. Sci. 22, 1017–1032.
Meinshausen, M., Smith, S.J., Calvin, K., Daniel, J.S., Kainuma, M.L.T., Lamarque, J.-F., Matsumoto, K., Montzka, S.A., Raper, S.C.B., Riahi, K., 2011. The RCP greenhouse gas concentrations and their extensions from 1765 to 2300. Clim. Change 109, 213.
Milly, P.C.D., Wetherald, R.T., Dunne, K.A., Delworth, T.L., 2002. Increasing risk of great floods in a changing climate [WWW Document]. Nature.
Mitchell, D., James, R., Forster, P.M., Betts, R.A., Shiogama, H., Allen, M., 2016. Realizing the impacts of a 1.5 C warmer world. Nat. Clim. Chang. 6, 735.
Pierce, D.W., Cayan, D.R., Thrasher, B.L., 2014. Statistical downscaling using localized constructed analogs (LOCA). J. Hydrometeorol. 15, 2558–2585.
Prat, O.P., Nelson, B.R., 2015. Evaluation of precipitation estimates over CONUS derived from satellite, radar, and rain gauge data sets at daily to annual scales (2002–2012). Hydrol. Earth Syst. Sci. 19, 2037.
Qin, Y., Abatzoglou, J.T., Siebert, S., Huning, L.S., AghaKouchak, A., Mankin, J.S., Hong, C., Tong, D., Davis, S.J., Mueller, N.D., 2020. Agricultural risks from changing snowmelt. Nat. Clim. Chang. 10, 459–465. https://doi.org/10.1038/s41558-020-0746-8
Rogelj, J., den Elzen, M., Höhne, N., Fransen, T., Fekete, H., Winkler, H., Schaeffer, R., Sha, F., Riahi, K., Meinshausen, M., 2016. Paris Agreement climate proposals need a boost to keep warming well below 2 °C. Nature 534, 631.
Sharma, S., Siddique, R., Reed, S., Ahnert, P., Mendoza, P., Mejia, A., 2018. Relative effects of statistical preprocessing and postprocessing on a regional hydrological ensemble prediction system. Hydrol. Earth Syst. Sci. 22. https://doi.org/10.5194/hess-22-1831-

2018
Siddique, R., Karmalkar, A., Fengyun., S., Palmer, R.N., 2020. Hydrological extremes across the Commonwealth of Massachusetts. J. Hydrol. Reg. Stud. Under Revi.
Siddique, R., Mejia, A., 2017. Ensemble Streamflow Forecasting across the US Mid-Atlantic Region with a Distributed Hydrological Model Forced by GEFS Reforecasts. J. Hydrometeorol. 18, 1905–1928.
Siddique, R., Mejia, A., Brown, J., Reed, S., Ahnert, P., 2015. Verification of precipitation forecasts from two numerical weather prediction models in the Middle Atlantic Region of the USA: A precursory analysis to hydrologic forecasting. J. Hydrol. 529. https://doi.org/10.1016/j.jhydrol.2015.08.042
Siddique, R., Palmer, R., 2020. Climate Change Impacts on Local Flood Risks in the U.S. Northeast: A Case Study on the Connecticut and Merrimack River Basins. JAWRA J. Am. Water Resour. Assoc. n/a. https://doi.org/10.1111/1752-1688.12886
Swain, S., Hayhoe, K., 2015. CMIP5 projected changes in spring and summer drought and wet conditions over North America. Clim. Dyn. 44, 2737–2750. https://doi.org/10.1007/s00382-014-2255-9
Taylor, K.E., Stouffer, R.J., Meehl, G.A., 2012. An overview of CMIP5 and the experiment design. Bull. Am. Meteorol. Soc. 93, 485–498.
UNFCCC, V., 2015. Adoption of the Paris agreement. United Nations Off. Geneva, Geneva Google Sch.
Van Loon, A.F., 2015. Hydrological drought explained. WIREs Water 2, 359–392. https://doi.org/10.1002/wat2.1085
Wood, A.W., Hopson, T., Newman, A., Brekke, L., Arnold, J., Clark, M., 2016. Quantifying streamflow forecast skill elasticity to initial condition and climate prediction skill. J. Hydrometeorol. 17, 651–668.
Yang, X., Sharma, S., Siddique, R., Greybush, S.J., Mejia, A., 2017. Postprocessing of GEFS precipitation ensemble reforecasts over the U.S. mid-atlantic region. Mon. Weather Rev. 145. https://doi.org/10.1175/MWR-D-16-0251.1
Zhang, J., Howard, K., Langston, C., Vasiloff, S., Kaney, B., Arthur, A., Van Cooten, S., Kelleher, K., Kitzmiller, D., Ding, F., 2011. National Mosaic and Multi-Sensor QPE (NMQ) system: Description, results, and future plans. Bull. Am. Meteorol. Soc. 92, 1321–1338.
Zhuan, M.-J., Chen, J., Shen, M.-X., Xu, C.-Y., Chen, H., Xiong, L.-H., 2018. Timing of human-induced climate change emergence from internal climate variability for hydrological impact studies. Hydrol. Res. 49, 421–437.